Contrib Mineral Petrol (2001) 141: 222–232
DOI 10.1007/s004100100238

Robert W. Luth

Experimental determination of the reaction aragonite + magnesite = dolomite at 5 to 9 GPa

Received: 1 May 2000 / Accepted: 11 December 2000 / Published online: 27 February 2001

Abstract Martinez et al. bracketed the decomposition reaction of dolomite to aragonite + magnesite between 5.0 and 5.5 GPa at 600 °C using in-situ XRD in a multi-anvil apparatus. They then extrapolated their results using the available thermodynamic data such that the breakdown reaction occurs at ~1,000 °C at 6 GPa. If correct, this extrapolation has implications for the type(s) of stable carbonate(s) in the mantle. For example, the reaction magnesite + diopside = dolomite + enstatite would be metastable at $P > 7$ GPa relative to the aragonite-containing analog, and thus aragonite, rather than dolomite, might be stable near the solidus of lherzolite. This extrapolation would also imply that aragonite and magnesite would be stable in garnet + clinopyroxene assemblages at pressures in the stability field of diamond. To test this extrapolation, experiments were conducted at higher temperatures in a multiple-anvil apparatus. Results of initial experiments were consistent with the results of Martinez et al. At higher temperatures, however, the reaction occurs at higher pressures than predicted by Martinez et al., requiring significant curvature to the reaction boundary. This curvature (increasing dP/dT with increasing T) is consistent with increasing disorder in the dolomite with increasing temperature, increasing the stability of dolomite relative to aragonite plus magnesite. The experimental results restrict aragonite + magnesite-bearing assemblages to low temperature. Aragonite will not be present in near-solidus lherzolite, and can be present in orthopyroxene-free eclogites and pyroxenites only at low temperature.

R. W. Luth
C. M. Scarfe Laboratory for Experimental Petrology,
Department of Earth and Atmospheric Sciences,
University of Alberta, Edmonton,
Alberta T6G 2E3, Canada
E-mail: robert.luth@ualberta.ca
Tel.: +1-780-4922740

Editorial responsibility: T. L. Grove

Introduction

Martinez et al. (1996) studied the high-pressure, high-temperature behavior of aragonite and dolomite with in situ XRD, using the SAM-85 DIA-type multiple-anvil apparatus on the X17B beam line at the National Synchrotron Light Source at Brookhaven National Laboratory. Their main interest was to determine the volume behavior of the carbonates with changing P and T, and to derive equations of state (EOS). They also found that dolomite broke down between 5 and 5.5 GPa at 600 °C to aragonite plus magnesite. By combining their EOS data, their experimental bracket on the decomposition reaction, and available thermodynamic data, the decomposition reaction was extrapolated to higher temperatures and pressures, such that the reaction would occur at ~1,000 °C at 6 GPa. This extrapolation, pinned to a single experimentally-determined P,T datum on the decomposition reaction, relies heavily on the quality of the thermodynamic data, and therefore Martinez et al. (1996) used several different data sets for their extrapolations. None of these data sets took into account the energetic effects of increasing disorder in dolomite with increasing temperature.

If correct, this extrapolation would preclude dolomite being stable at near-solidus temperatures in peridotite, because aragonite (± magnesite) would be stable instead. Dolomite is stable in peridotite on the low-pressure side of the reaction $CaMgSi_2O_6$(di) + 2 $MgCO_3$(mag) = $Mg_2Si_2O_6$(en) + $CaMg(CO_3)_2$(dol) (Brey et al. 1986). The existence of the dolomite decomposition reaction requires that this exchange reaction would terminate at an invariant point involving diopside, enstatite, magnesite, dolomite and aragonite. The thermodynamic database available at the beginning of this project (THERMOCALC v2.4, Holland and Powell 1990) predicts this invariant point to occur at ~5.6 GPa and ~1,280 °C (Fig. 1). It must be noted explicitly that this calculation extrapolates the thermodynamic database to significantly higher pressures than those at

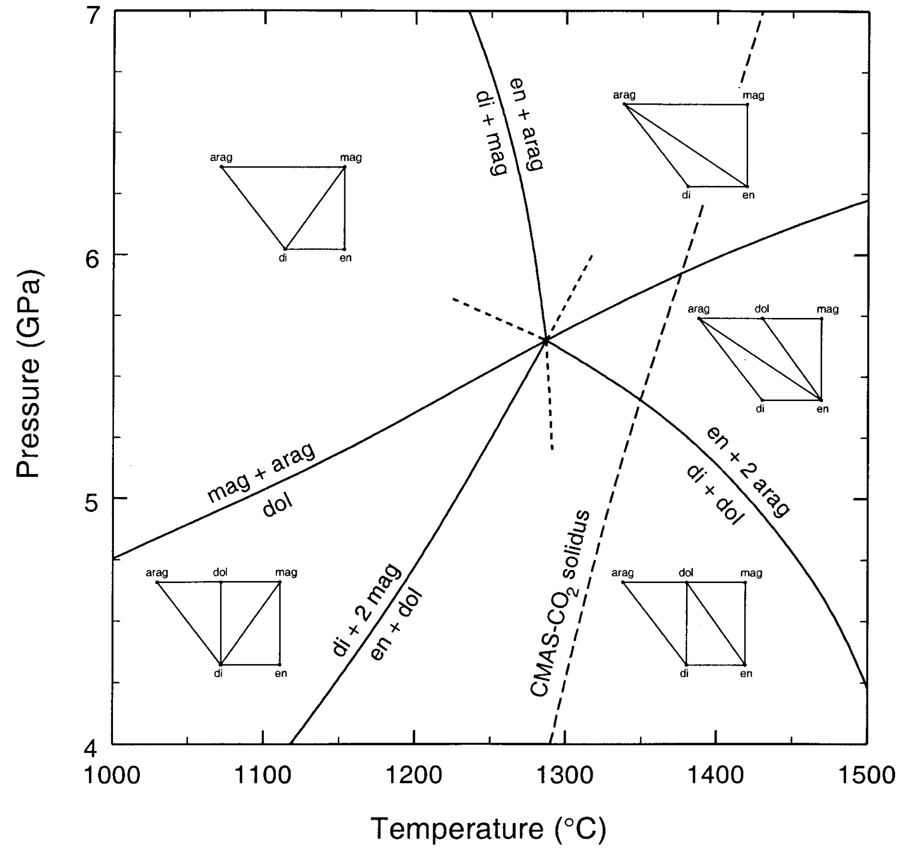

Fig. 1 Schreinemaker's analysis of the distribution of univariant reactions about the invariant point (en, di, arag, mag, dol) in the system CaO–MgO–SiO_2–CO_2. There is compositional degeneracy in this system; these phases are all coplanar in this composition space, reducing the effective number of components to 3 (e.g., $CaSiO_3$–$MgSiO_3$–$Si_{-1}C$). The CMAS–CO_2 solidus shown is for the assemblage fo + en + di + gar + carbonate from Dalton and Presnall (1998)

which it is calibrated. For reference, Fig. 1 also shows the experimentally-determined univariant solidus in the system CMAS–CO_2 involving the assemblage fo + en + di + gar + carbonate (Dalton and Presnall 1998), which should be displaced to lower temperatures relative to the solidus for the assemblage fo + en + di + carbonate in the CMS–CO_2 system. The compatibility diagrams in Fig. 1 (inset) show how the possible carbonates coexisting with pyroxenes change upon crossing the reactions around this invariant point. The carbonate(s) present at near-solidus conditions in peridotite would depend on the ratio of orthopyroxene to clinopyroxene, and on the amount of carbonate present.

A further implication of this extrapolation of the dolomite decomposition reaction is that aragonite (± magnesite) would be the carbonate found in metabasaltic-composition eclogites, rather than dolomite. If correct, this would affect the carbon–carbonate–silicate reactions that may control the stability of diamond in mantle eclogite (Luth 1993), requiring a re-evaluation of these reactions.

Because of all these implications, this reaction needed to be determined experimentally at higher temperatures.

Experimental

All experiments used as starting material natural dolomite from Eugui, Spain, which was used in a previous study of the reaction dolomite + 2 coesite = diopside + 2 CO_2 (Luth 1995). Dolomite from this locality has been used extensively for crystallographic, TEM, and calorimetric studies (Reeder and Wenk 1983; Reeder and Nakajima 1982; Navrotsky and Capabianco 1987; Chai and Navrotsky 1996; Navrotsky et al. 1999). A second series of experiments was conducted on an equimolar mixture of Eugui dolomite, natural magnesite from Mt. Brussilof, British Columbia, Canada, and synthetic aragonite. The aragonite was crystallized from $CaCO_3$ (Alfa 99.95%) at 3 GPa, 800 °C in a sealed Pt capsule in a piston-cylinder apparatus. The powder X-ray diffractogram of the run product contained only aragonite peaks.

For the high-pressure experiments, the samples were encapsulated in triple-crimped, welded Pt capsules of 1.5 mm OD. Approximately 3–5 mg of sample was loaded, the capsule was dried at 120 °C for at least 16 h, then the top of the capsule was welded shut. The sealed capsule was compressed gently into a compact cylinder in a steel die. The capsules were run in sample assemblies consisting of a semi-sintered MgO + 5% Cr_2O_3 octahedron of 18-mm edge length containing a stepped graphite furnace surrounded by a ZrO_2 sleeve, inner MgO spacers, and an axial $W_{95}Re_5$–$W_{74}Re_{26}$ thermocouple housed in an alumina (99.98%) sleeve, as previously used by Walter et al. (1994), Luth (1995), and Knoche et al. (1999). The pressure calibration was based on experimental brackets at 1,000 °C of the quartz-coesite transition in SiO_2 at 2.95 GPa (Bohlen 1984), the garnet–perovskite transition in $CaGeO_3$ at 6.1 GPa (Susaki et al. 1985), and the coesite–

stishovite transition in SiO_2 at 9.1 GPa (Yagi and Akimoto 1976), as detailed in Walter et al. (1994). The uncertainty in pressure is estimated to be ± 0.5 GPa based on the reproducibility of the calibration experiments. All experiments were run in the USSA-2000 split-sphere multiple-anvil apparatus in the CM Scarfe Laboratory for Experimental Petrology at the University of Alberta.

Experiments were brought to run pressure, then heated at ~70 °C/min to run temperature, and maintained at ± 5 °C. No correction for pressure was applied to the emf of the thermocouple. Temperature gradients within the sample capsule are estimated to be < 50 °C, based on two-pyroxene geothermometry (Domanik and Luth 1999).

Some two-stage experiments were conducted to test for equilibrium. In these experiments, the first stage used the above procedure, and was run at conditions known from previous experiments to be on the low-temperature side of the reaction, where aragonite + magnesite is stable. After the equilibration period at that temperature, the experiment was heated to a higher temperature at the same pressure, and allowed to equilibrate at those conditions, which from previous experiments were on the high-temperature (dolomite-stable) side of the reaction.

The experiments were quenched by turning off the power to the furnace, resulting in a temperature drop to < 300 °C in 2–5 s. The experiment was then decompressed over 3–6 h, depending on the pressure of the experiment. The majority of each experimental run product, once extracted from the capsule, was ground in an agate mortar and pestle, and analyzed with powder X-ray diffraction. A portion of each run product was reserved for possible analysis by electron microprobe. Selected samples were mounted in epoxy plugs, ground and polished for analysis with a JEOL 8900R electron microprobe. The textural relationships between the phases present were imaged using back-scattered electron (BSE) imaging, and quantitative analysis was done on samples with > 5 μm grain size. The quantitative analyses were done at 15 kV accelerating voltage and 5 nA sample current as measured on a Faraday cup. Carbonate standards were used, and the data were reduced with the ZAF correction scheme provided by JEOL. Carbon (as carbonate) was calculated by stoichiometry.

Results

The results of the experiments, based on powder XRD, are shown in a P–T projection in Fig. 2 and are tabulated in Table 1, which also lists the relative intensities of the most intense peak for each phase in the powder X-ray diffractogram. Although these values are not quantitative measures of proportions of phases, they do indicate relative abundances.

The initial results at low temperature (627 °C) bracketed the reaction at 5–5.5 GPa, consistent with the results of Martinez et al. (1996). At higher temperatures, dolomite was stable at higher pressures than predicted, and the reaction boundary was found to be curved (Fig. 2) with a significant change in slope at ~900 °C.

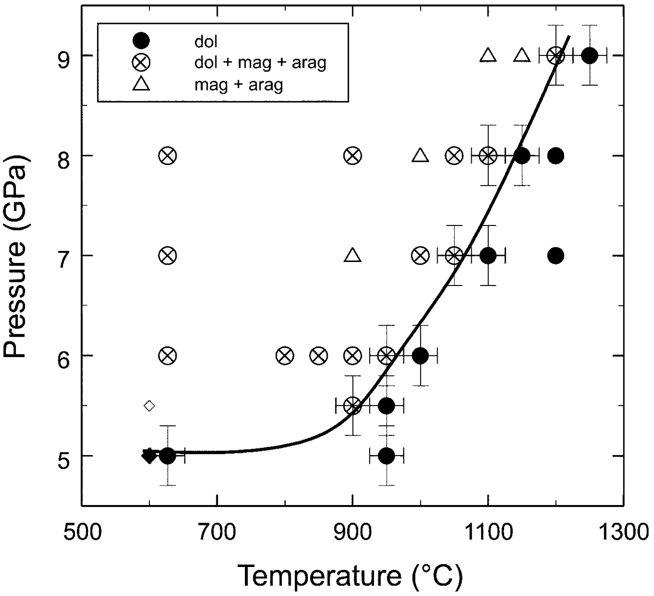

Fig. 2 Experimental results of dolomite breakdown experiments. *Error bars* are estimated uncertainties; they are shown only on the data points defining the reaction boundary for clarity. *Solid line* is a visual fit to the data

As seen in Fig. 2, there is a substantial range of temperature–pressure space over which aragonite, magnesite, and dolomite coexist, in violation of the Gibbs Phase Rule for a two component system. One possible explanation for this result is that the charges were zoned because of temperature gradients, such that the lower-temperature regions were magnesite plus aragonite and the higher-temperature region was dolomite. The thermal gradients in these experiments is < 50 °C (Domanik and Luth 1999), which is insufficient to explain the large temperature region over which the three-phase assemblage is observed in the XRD data. To test this possibility further, two additional experiments were conducted at P, T conditions where all three phases were present (runs 1491, 1492; Table 1). The capsules from these experiments were embedded in epoxy, ground down to expose a longitudinal cross section of the sample, and imaged with BSE on the electron microprobe. In both cases, the three phases coexist throughout the charge, and the textural relationships are consistent with metastable persistence of dolomite (see below). These results are consistent with those of Buob and Ulmer (2000), who found no evidence of thermal zoning in their experiments on this reaction (Ulmer, personal communication 2000). Based on these results, and the results of time series experiments (e.g., runs 1344 and 1406 at 8 GPa, 627 °C, and 1409 and 1434 at 8 GPa, 1,100 °C), the most reasonable explanation for the apparent violation of the Phase Rule is that this reaction is kinetically hindered. This explanation is supported by the observation that the abundances of magnesite and

Table 1 Experimental results. *dol* Dolomite; *mag* magnesite; *arag* aragonite. Numbers in parentheses in Results column are X_{Mg} ($=\mathrm{Mg}/(\mathrm{Mg}+\mathrm{Ca})$) on a cation basis as determined by electron microprobe. Intensity ratios: relative intensities of most intense peak for each carbonate: (104) for dolomite and magnesite, (111) for aragonite. *n.x.* Not X-rayed; whole capsule mounted for electron microprobe analysis to test for spatial distribution of arag + mag versus dol

Run no.	P (GPa)	T (°C)	Time (h)	Results	Intensity ratio (dol:arag:mag)
Starting material: dolomite					
1411	5	627	24	dol + arag + mag	100:1:2
1440	5	950	24	dol	100:0:0
1436	5.5	900	24	dol + arag + mag	100:5:10
1444	5.5	950	24	dol	100:0:0
1407	6	627	24	dol + arag + mag	100:7:9
1418	6	800	24	dol + arag + mag	100:4:9
1421	6	850	24	dol + arag + mag	100:24:42
1423	6	900	24	dol + arag + mag	100:9:19
1491	6	900	24	dol + arag + mag	n.x.
1424	6	950	24	dol (0.494) + arag (0.003) + mag (0.959)	45:50:100
1433	6	1,000	24	dol	100:0:0
1342	7	627	6	dol + arag + mag	100:6:6
1408	7	627	24	dol + arag + mag	100:15:17
1413	7	900	21	arag + mag	0:59:100
1420	7	1,000	12	dol + arag + mag	100:11:24
1422	7	1,050	24	dol (0.492) + arag (0.002) + mag (0.942)	18:56:100
1425	7	1,100	24	dol	100:0:0
1445	7	1,050	24		
		→1,100	24	dol + arag + mag	100:24:48
1330	7	1,200	6	dol	100:0:0
1343	8	627	6	dol	100:0:0
1344	8	627	6	dol + arag + mag	100:2:3
1406	8	627	24	dol + arag + mag	93:70:100
1341	8	900	6	dol + arag + mag	100:48:71
1410	8	1,000	12	arag (0.001) + mag (0.944)	0:53:100
1412	8	1,050	12	dol + arag + mag	100:11:16
1492	8	1,050	24	dol + arag + mag	n.x.
1409	8	1,100	8	dol + mag	100:0:1
1434	8	1,100	24	dol + arag + mag	14:57:100
1438	8	1,150	24	dol	100:0:0
1340	8	1,200	6	dol	100:0:0
1427	9	1,100	24	arag + mag	0:55:100
1435	9	1,150	24	dol + arag + mag	7:46:100
1441	9	1,200	24	dol + arag + mag	100:2:2
1442	9	1,250	24	dol	100:0:0
Starting Material: dolomite + aragonite + magnesite					
1527	6	900	24	dol + arag + mag	100:21:31
1528	6	900	48	dol + arag + mag	3:53:100
1529	6	950	24	dol + mag	100:0:4
1530	6	900	48		
		→1,000	24	dol + mag	100:0:3
1531	6	900	48		
		→950	24	dol + arag + mag	22:63:100

aragonite relative to dolomite (as judged from XRD intensities) decrease with decreasing temperature at constant run time, rather than increasing as would be expected by moving further into the stability field for magnesite + aragonite (cf. 6 GPa results at 900 and 950 °C, runs 1423 and 1424, respectively, Table 1).

Backscattered electron imaging of selected run products show that the dolomite breaks down in a eutectoid fashion into a very fine-scale intergrowth of aragonite plus magnesite (Fig. 3a), commonly with residual dolomite. Coarsening to grain sizes amenable to electron microprobe analysis occurs only very close to the reaction boundary, at least on the time scales of these experiments (Fig. 3b). Further away from the reaction boundary, the run product may consist entirely of vermicular aragonite + magnesite intergrowth (Fig. 3c) but with no significant coarsening. At temperatures above the reaction boundary, dolomite is present (Fig. 3d), with no textural evidence of reaction or exsolution.

Two experiments at 8 GPa, 1,100 °C for different durations illustrate some of the kinetic problems associated with determining this reaction boundary. After 8 h, the stoichiometric dolomite starting material has formed a small amount of magnesite and (by mass balance) a Ca-enriched dolomite solid solution (Fig. 4a). This result is consistent with stoichiometric dolomite being metastable relative to magnesite plus dolomite with $\mathrm{Ca}/\mathrm{Mg} > 1$. With a longer run duration, however, the magnesite plus Ca-rich dolomite assemblage reacts in turn to form aragonite and magnesite surrounding

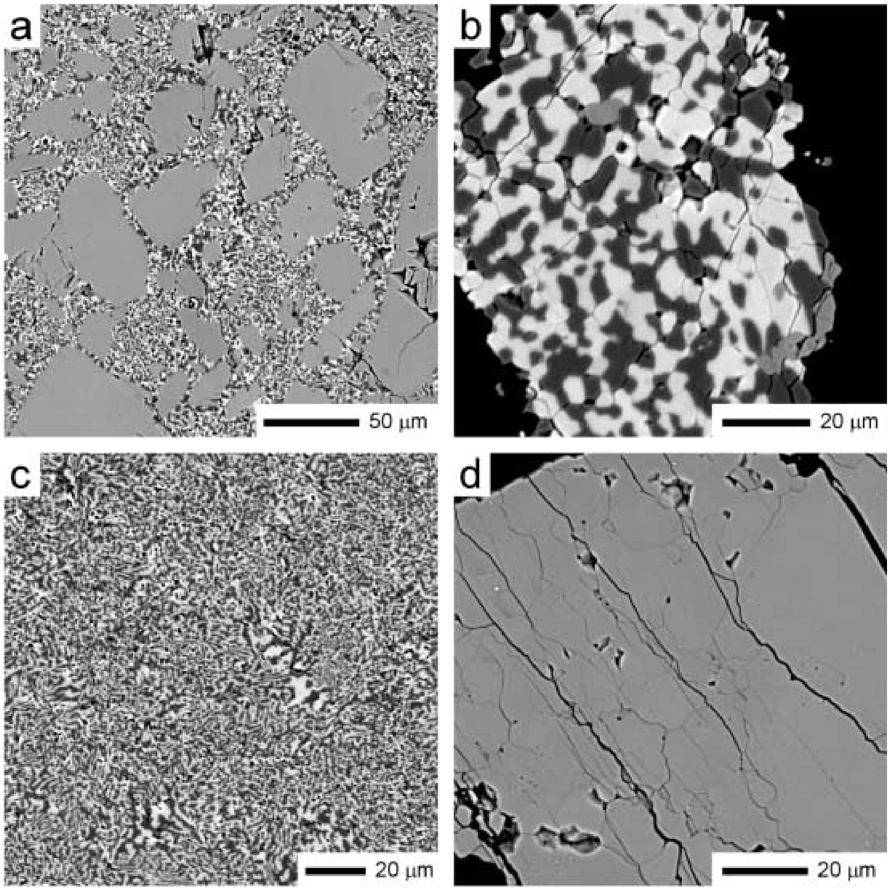

Fig. 3 Backscattered electron images of run products. See text for discussion. **a** #1423: 6 GPa, 900 °C, 24 h. Large grains of dolomite (*medium gray*) surrounded by eutectoid intergrowth of magnesite (*dark gray*) and aragonite (*light gray*). **b** #1424: 6 GPa, 950 °C, 24 h. Granular intergrowth of aragonite (*light gray*), magnesite (*dark gray*), and residual dolomite (*medium gray*). **c** #1413: 7 GPa, 900 °C, 21 h. Eutectoid intergrowth of aragonite (*light gray*) and magnesite (*dark gray*). No dolomite present. **d** #1438: 8 GPa, 1,150 °C, 24 h. Massive dolomite. No aragonite or magnesite

relict dolomite (Fig. 4b). This stepwise reaction behavior requires that the Ca-rich dolomite plus magnesite assemblage, although more stable than stoichiometric dolomite, be metastable relative to the assemblage of aragonite and magnesite solid solutions.

The BSE images are very useful in confirming the direction of reaction inferred from the powder XRD results. In single-stage experiments at 7 GPa, dolomite is stable at 1,100 °C, and relatively coarse-grained aragonite + magnesite (Fig. 4c) coexist with small amounts of residual dolomite (not shown; seen elsewhere and in the X-ray diffractogram) at 1,050 °C. In a two-stage experiment (1445) at 7 GPa, with the first stage at 1,050 °C and the second at 1,100 °C, dolomite is present in a fine-scale intergrowth with aragonite and magnesite (Fig. 4d): a texture that contrasts with the clearly residual nature of dolomite in experiments in the aragonite + magnesite stability field (Figs. 3a and 4b). Thus, dolomite is interpreted to be growing at the expense of magnesite + aragonite during the 1,100 °C stage of this experiment.

Discussion

Equilibrium?

To what extent do these results approach equilibrium? Experiments that start with dolomite only may overestimate the stability field for dolomite if nucleation of aragonite and/or magnesite is inhibited. The result of the two-stage experiment (run 1445, Table 1) is consistent with the results of single-stage experiments, which would not be the case if these experiments had exaggerated the stability field of dolomite.

To provide constraints on the reaction boundary from a different perspective, additional experiments were conducted using a starting material containing dolomite, pure magnesite, and pure aragonite. The results of these experiments (Table 1) bracket the reaction boundary at 6 GPa between 900 and 950 °C, compared with the 950–1,000 °C bracket from the experiments using only dolomite as a starting material. The aragonite + magnesite + dolomite starting material is not ideal, because pure aragonite and magnesite are metastable relative to their solid-solution counterparts at the reaction boundary. The behavior of this starting material may then depend on the kinetics of the exchange of cations between coexisting carbonates to form the stable solid solutions, relative to recrystallization or reaction of the end member aragonite and magnesite to form dolomite. For example, at temperatures just below the reaction boundary, dolomite might be less metastable than the assemblage of end member aragonite + magnesite. Under these conditions, the pure aragonite and magnesite in the starting material could react to form more dolomite rather than exchange cations to form the stable

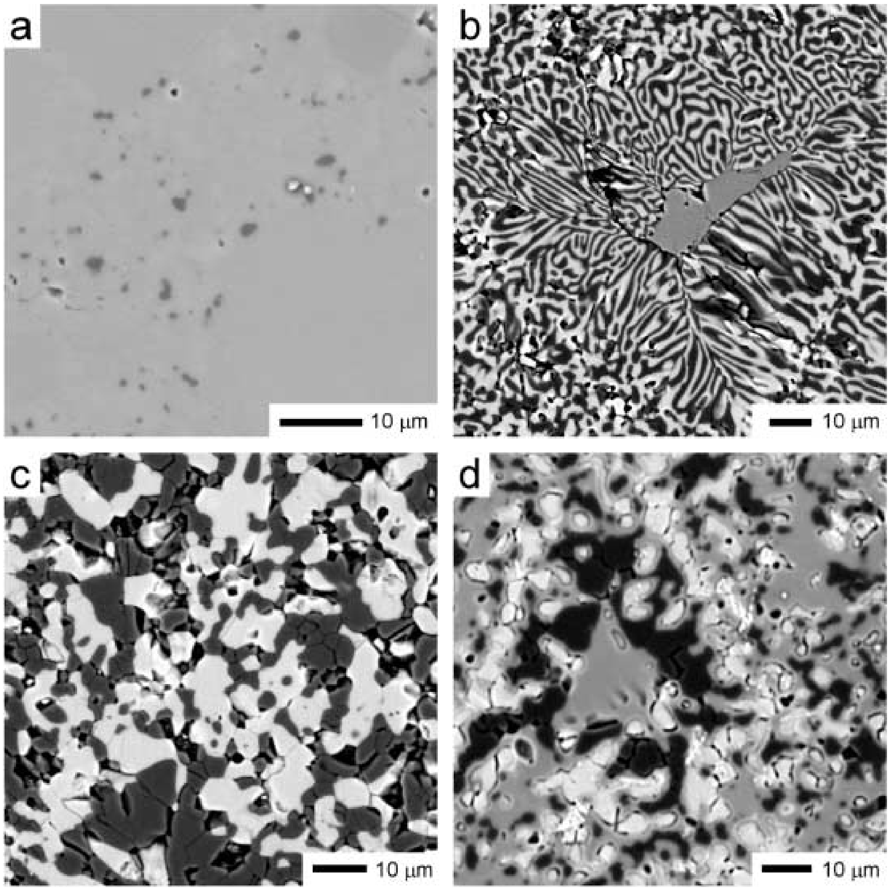

Fig. 4 Backscattered electron images of run products. See text for discussion. **a** #1409: 8 GPa, 1,100 °C, 8 h. Dolomite (*medium gray*) with small crystals of magnesite (*dark gray*). No aragonite is present. **b** #1434: 8 GPa, 1,100 °C, 24 h. Eutectoid intergrowth of aragonite (*light gray*) and magnesite (*dark gray*) surrounding residual grain of dolomite (center, medium gray). **c** #1422: 7 GPa, 1,050 °C, 24 h. Granular intergrowth of aragonite (*light gray*) and magnesite (*dark gray*). Small amount of residual dolomite was observed in other parts of this run product. **d** #1445: 7 GPa. 1,050 °C, 24 h→1,100 °C, 24 h. Grains of aragonite (*light gray*) and magnesite (*dark gray*) that grew in first stage of the experiment (at 1,050 °C), surrounded by dolomite (*medium gray*) grown in second stage of the experiment (at 1,100 °C). Interpretation: Dolomite is forming at the expense of aragonite + magnesite

solid-solution aragonite + magnesite (Fig. 5), if the kinetics of recrystallization are faster than inter-carbonate cationic exchange. This scenario might explain the lower temperature bracket found for the dolomite + magnesite + aragonite starting material compared with the dolomite-only starting material.

To test this possibility, two-stage experiments (1530, 1531; Table 1) were conducted. The first of these (1530) clearly brackets the reaction boundary. Although the run product of 1531 contained all three phases, there was an increase in dolomite relative to the run product of the single stage experiment at 900 °C (1528), judging from the relative intensities of the dolomite peaks in the diffractogram (Table 1). This result is taken as evidence that dolomite grew in the second stage of 1531 (at 950 °C), and hence the 900–950 °C bracket is valid. The difference between this result and that for the dolomite-only starting material is therefore attributed to experimental uncertainty.

Comparison with previous work

The results of the present study are consistent with the results of Liu and Lin (1995), who found dolomite broke down between 6 and 7 GPa at ~1,000 °C in a diamond-anvil cell. Buob and Ulmer (2000) determined the breakdown reaction to occur between 5 and 6 GPa at 800 °C, and between 6 and 7 GPa at 1,000 °C, consistent with the results of the present study. In contrast to the present results, however, these authors reported complete miscibility between aragonite and dolomite above 1,100 °C, implying the breakdown reaction would terminate at 1,100 °C. In light of the higher-pressure results in this study, in which aragonite and magnesite coexist, the reason for this discrepancy is not apparent.

Comparison with calculated curves

The reaction boundaries calculated by Martinez et al. (1996) and with THERMOCALC version 2.4 (Holland and Powell 1990) are nearly linear and subparallel to the low-temperature portion of the experimental reaction boundary (Fig. 6). Neither calculated curve shows the curvature required by the new experimental data. The curve calculated with a newer version of Holland and Powell's database (THERMOCALC version 2.7) has a generally steeper slope, consistent with the slope of the high-temperature part of the experimental curve (TC2.7 on Fig. 6), and does increase dP/dT with increasing P, but not to the extent seen in the experiments. The database of Chatterjee et al. (1998) produces a curve that is slightly more curved and in agreement with the experimental data at > 800 °C. Neither this curve, nor that of THERMOCALC 2.7, agree with the lower-temperature data of Martinez et al. (1996).

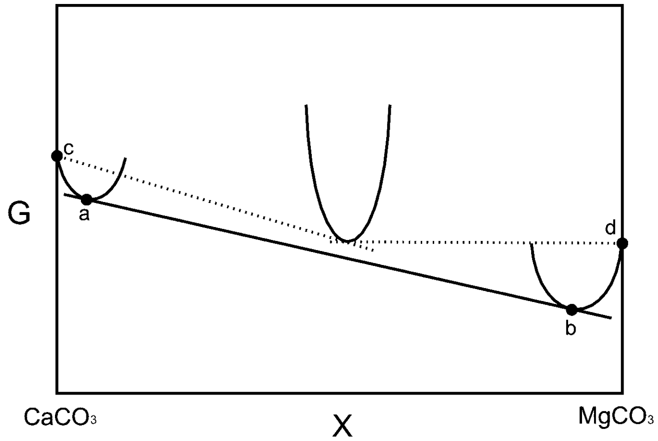

Fig. 5 Schematic section of possible free energy–composition relationships at conditions on the low-T side of the reaction boundary. The curves are schematic G-X expressions for the three carbonate solid solutions. The stable assemblage underthese conditions consists of **a** aragonite solid solution and **b** magnesite solid solution. However, dolomite is less metastable than **c** a mechanical mixture of end member aragonite and **d** end member magnesite. Therefore, metastable dolomite solid solutions could form in preference to reaction of the end members to form the stable solid solution assemblage

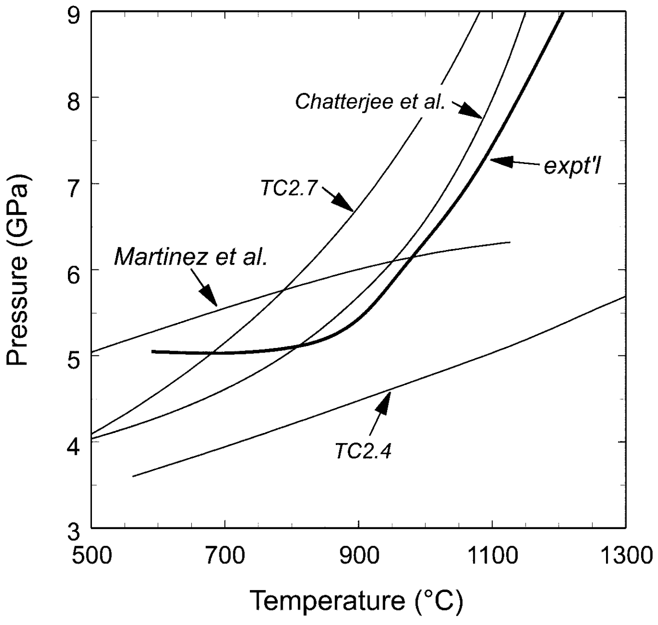

Fig. 6 Comparison of experimental results (*heavy line*) with that calculated by Martinez et al. (1996) and with those calculated with THERMOCALC v.2.4 (Holland and Powell 1990), THERMOCALC v.2.7 (Holland and Powell 1998), and BAYES (Chatterjee et al. 1998, program version dated 2/23/98)

Cause(s) of curvature

From the Clapeyron equation, the change in curvature of this reaction boundary may result from changes in ΔH_{rxn}, ΔV_{rxn}, or both. Any change in ΔV_{rxn} results from differing compressibilities of the carbonates. This effect may be calculated from the equation of states for dolomite and aragonite from Martinez et al. (1996), and for magnesite from Zhang et al. (1997). The ΔV_{rxn} decreases with increasing pressure (Table 2), which would increase the slope of the reaction boundary if ΔS_{rxn} remained constant. This effect by itself would only increase the slope by ~50%, however, rather than the > 2,000% required by the experimental data.

Increasing thermal disorder in dolomite with increasing temperature would tend to stabilize dolomite relative to magnesite + aragonite with increasing temperature. Therefore, the consequences of disorder must be evaluated to estimate its effect on the curvature of the reaction boundary.

Degree of order in dolomite

The structure of dolomite may be viewed as a derivative of the calcite structure, in which layers of Ca cations alternate with layers of carbonate anions. In ordered dolomite, every other layer of Ca cations is replaced with a layer of Mg cations. In disordered dolomite, each cation layer has a random mixture of 50% Ca and 50% Mg cations. This disordering occurs gradually with increasing temperature, and can be quantified by a "degree of order" parameter, *S*, that varies from zero (complete disorder) to one (complete order). Single-crystal X-ray diffraction studies have been used to quantify the degree of order in thermally-disordered samples (Reeder and Wenk 1983). Among other results, these authors found that completely disordered samples could not be recovered because they tended to re-order upon quenching. Because of this problem, any post-experiment measurement of *S* provides only an upper bound on its value.

Because the present experiments used powdered samples, single-crystal studies were not feasible, and constraints from the powder XRD data were needed. A powder X-ray diffractogram of ordered dolomite has peaks from (101), (015), and (021) reflections, which are absent in diffractograms of the disordered carbonate (Goldsmith and Heard 1961). Therefore, an initial con-

Table 2 Calculations bearing on the slope of the reaction boundary

P (GPa)	T (°C)	ΔV_{rxn} (J/bar)	Slope (bar/°C)	ΔH (kJ)	ΔH_{P}–$\Delta H_{5\ \mathrm{GPa}}$ (kJ)
5.0	600	0.1900	1.64	0.27	0.00
6.0	0980	0.1482	93.03	16.55	16.28
7.0	1,075	0.1390	116.88	20.90	20.63
8.0	1,140	0.1331	149.53	26.93	26.66

Table 3 Intensities of dolomite reflections for samples with I_{104} > 1000 counts

Run no.	P, T, t	104	006	101	015	021	I_{015}/I_{006}
SM		9,206	462	176	427	148	0.92
1411	5, 627, 24	1,342	78	25	43	30	0.55
1440	5, 950, 24	4,508	203	37	145	56	0.71
1436	5.5, 900, 24	4,242	157	13	92	36	0.59
1444	5.5, 950, 24	4,115	220	45	142	71	0.65
1407	6, 627, 24	2,410	114	35	77	36	0.68
1418	6, 800, 24	2,050	68	18	36	34	0.53
1421	6, 850, 24	1,292	74	10	40	22	0.54
1423	6, 900, 24	2,547	138	17	99	50	0.72
1433	6, 1,000, 24	4,583	258	49	116	72	0.45
1342	7, 627, 6	2,306	101	21	63	47	0.62
1420	7, 1,000, 12	2,232	160	24	81	37	0.51
1445	7, 1,050→1,100, 24→24	1,529	110	8	10	5	0.09
1425	7, 1,100, 24	4,572	290	11	16	10	0.05
1330	7, 1,200, 6	3,571	223	10	13	10	0
1343	8, 627, 6	3,753	125	41	76	43	0.61
1344	8, 627, 6	2,826	181	32	78	66	0.43
1412	8, 1,050, 12	1,844	67	0	38	12	0.57
1409	8, 1,100, 8	2,609	109	5	15	15	0
1438	8, 1,150, 24	4,858	225	5	0	0	0
1340	8, 1,200, 6	4,736	391	15	15	10	0
1441	9, 1,200, 24	7,417	388	22	35	18	0.09
1442	9, 1,250, 24	4,853	220	0	0	0	0
Dolomite + aragonite + magnesite starting material							
1527	6, 900, 24	1,583	105	21	66	43	0.63
1529	6, 950, 24	2,287	110	35	84	71	0.76
1530	6, 900→1,000, 48→24	1,994	108	21	65	48	0.60

straint on the state of order of the dolomite comes from the presence or absence of these reflections (Table 3). These order reflections have low intensities in the diffractogram, so Table 3 lists only those experiments with sufficient dolomite [as judged by the intensity of the (104) reflection] to minimize errors in measuring intensities of very small peaks. At 7 and 8 GPa, where there are the best constraints, there is complete disorder at ≥1,100 °C. This value may be compared with the value of 1,150–1,200 °C estimated by Goldsmith and Heard (1961) based on results of experiments at ≤ 1 GPa. They also found that the temperature of complete disorder was lower for dolomite with Ca/Mg > 1. Reeder and Wenk (1983) determined a critical temperature of complete disorder of the value of 1,150 °C based on samples run at 1.1 and 2.0 GPa. There may be a slight decrease in the critical temperature with increasing pressure. If confirmed, this would be consistent with a small negative volume of disordering (Hazen and Navrotsky 1996).

The state of order in partially-disordered samples was assessed by measuring the change of intensity of the ordering peaks with increasing temperature. Schultz-Güttler (1986) used the ratio of the intensities of the (015) and (006) peaks as a measure of the degree of ordering. The (015) reflection is the most intense of the order reflections, the intensity of the (006) reflection is not affected by order/disorder, and the two are nearby such that no corrections are required to be able to compare their intensities. Applying this technique to the Eugui dolomite starting material, the resultant degree of order is 0.92, rather than 1.0, which suggests a precision of no better than 8% relative. Application of this technique to run products (Table 3) resulted in considerable scatter in the results at a given temperature. This scatter may result from variable amounts of re-ordering upon quenching, or from differing amounts of preferred orientation of the powders, which changes the intensity ratio independent of the degree of ordering. Another possible complication is that dolomite that is reacting to form aragonite and magnesite may not preserve an equilibrium state of order for that P and T. Even the data from experiments within the dolomite stability field are scattered (e.g., values of S from 0.65–0.76 at 950 °C, and 0.45–0.6 at 1,000 °C). This scatter is not pressure-related; both 1,000 °C experiments were at 6 GPa, and no systematic trend is seen in S with increasing pressure at 950 °C. In any event, the results were not considered to be quantitative, although there is a general trend to decreasing S with increasing temperature, as expected (Fig. 7).

For comparison, Goldsmith and Heard (1961) found no detectable weakening of the order reflections in experiments quenched from below ~1,000 °C. Reeder and Wenk (1983) report values of S of 0.852 and 0.755 for experiments quenched from 1,050 °C, 1.1 GPa, and 1,100 °C, 1.1 GPa, respectively. Both of these studies point to preservation of order to higher temperatures than derived from the powder data in the present study, which may reflect a systematic underestimation of S by the method of Schultz-Güttler (1986). The 0.92 value derived for the Eugui dolomite starting material supports this possibility.

Landau-style (Putnis 1992; Holland and Powell 1998) and generalized point approximation/cluster variation

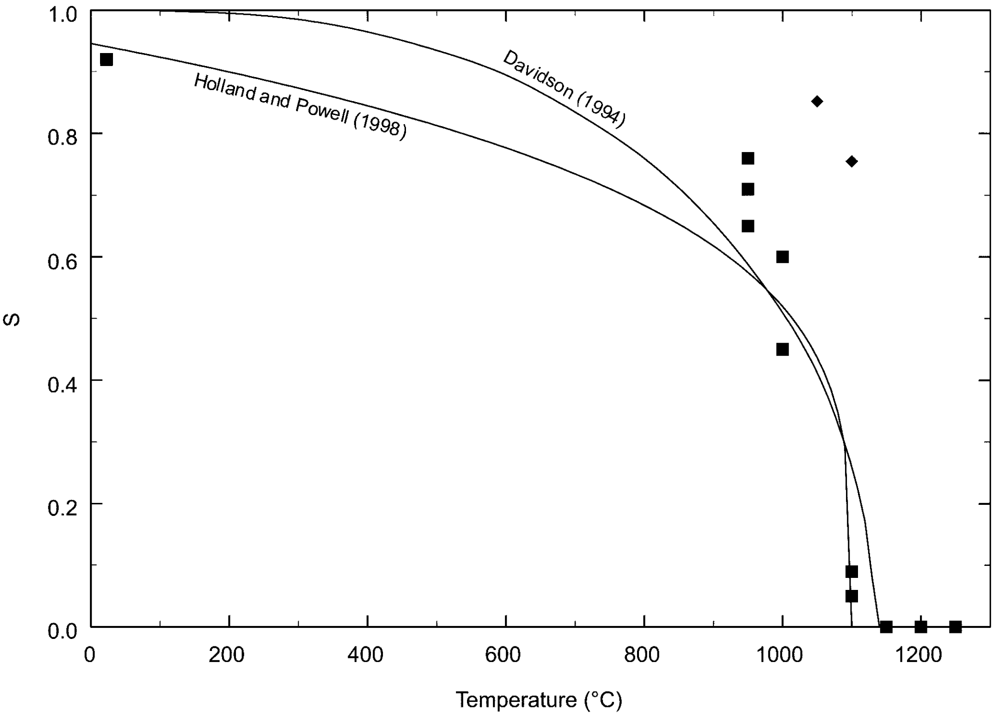

Fig. 7 Comparison of calculated degrees of order in $CaMg(CO_3)_2$ with temperature. Completely ordered dolomite has order parameter $S = 1$, completely disordered dolomite would have $S = 0$. Calculated curves show the results from the Landau-style model of Holland and Powell (1998) and the GPA model of Davidson (1994). *Filled squares* are estimates of S from experiments within the dolomite stability field (Table 3), calculated as discussed in text. *Filled diamonds* are values from Reeder and Wenk (1983) based on single-crystal XRD refinements on experimentally-disordered samples

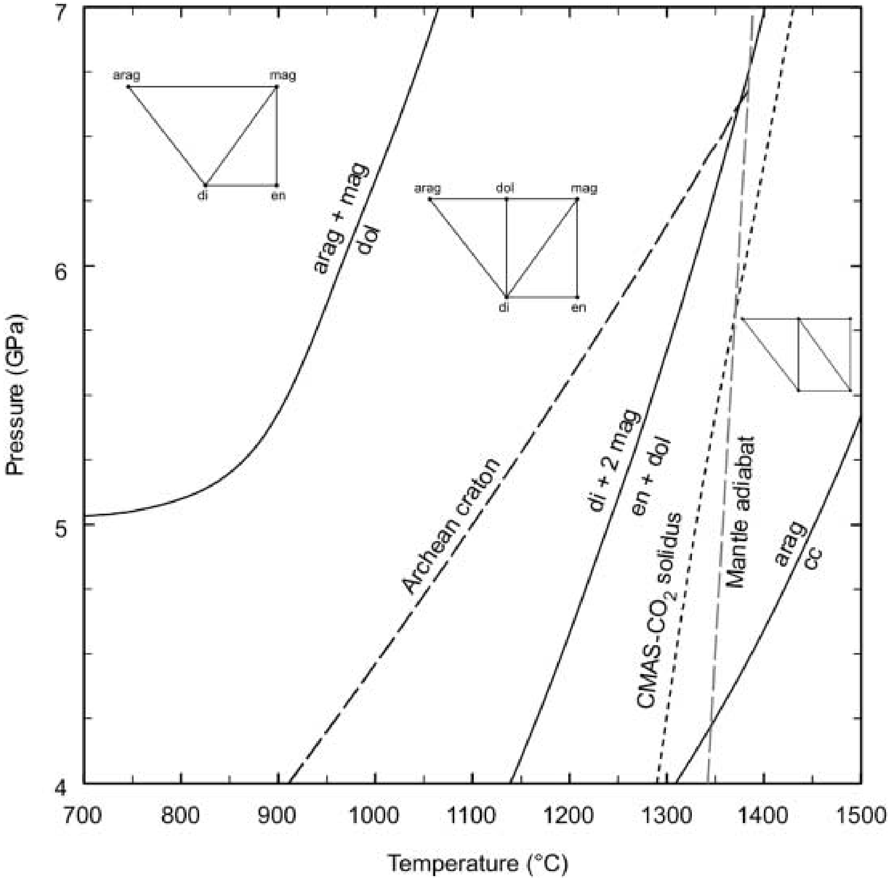

Fig. 8 Stable carbonates coexisting with clinopyroxene and orthopyroxene. Aragonite will not coexist with orthopyroxene-rich assemblages, only with clinopyroxene-bearing assemblages, and only then at low temperatures. Experimental dolomite decomposition reaction shown, other two curves calculated with THERMOCALC v.2.7 (Holland and Powell 1998). For reference, the CMAS–CO_2 solidus for peridotite of Dalton and Presnall (1998) is shown, as are an Archean craton geotherm and an average mantle adiabat from McKenzie and Bickle (1988)

method models (Davidson 1994) have been applied to the disordering behavior of (Ca, Mg)CO_3 carbonates. Both types of models predict disordering to occur over a range in temperature (Fig. 7). The quantitative application of these models to disordering in $CaMg(CO_3)_2$ has been handicapped by the re-ordering that occurs upon quenching, and the absence of in-situ studies of the degree of order. The values of *S* inferred from the powder XRD results of the run products in this study (Table 3) are in reasonable agreement with the models (filled squares, Fig. 7), given that the data only provide upper bounds on the values of *S*. In contrast, the previous studies of Goldsmith and Heard (1961) and Reeder and Wenk (1983) are consistent with a smaller temperature interval over which disordering takes place. That these models may predict the onset of disordering at too low a temperature is supported by the results of Capiobianco et al. (1987) in the analog $CdMg(CO_3)_2$ system, where disordering is not detected until much closer to the critical temperature than predicted by GPA models.

Effect of disorder on curvature

Can the observed curvature be explained by a model in which the shallow slope, low P, T part of the boundary curve involves ordered dolomite, and the steep slope, high P, T part of the boundary involves disordered dolomite? This model may be tested by application of the Clapeyron equation. By combining the dP/dT of the experimental reaction boundary at different pressures, the ΔV_{rxn} calculated above (Table 2), and the temperature at the reaction boundary, a ΔH_{rxn} may be obtained. This ΔH_{rxn} may be expressed as:

$$\Delta H_{rxn} = H_{\text{ordered dolomite}} + \Delta H_{\text{disorder, dolomite}} - H_{\text{aragonite}} - H_{\text{magnesite}}$$

At 5 GPa, the derived ΔH_{rxn} can be taken as $H_{\text{ordered dolomite}}-H_{\text{aragonite}}-H_{\text{magnesite}}$, given the assumption that the reaction at 5 GPa involves ordered dolomite. Therefore, the difference between the ΔH_{rxn} calculated for higher pressures and the ΔH_{rxn} at 5 GPa is $\Delta H_{\text{disorder, dolomite}}$. This calculated $\Delta H_{\text{disorder, dolomite}}$ must be corrected for the temperature effect on the enthalpy of the phases involved in the reaction; the corrected values are given in Table 2. Based on the change in slope of the experimental curve, $\Delta H_{\text{disorder,dolomite}}$ is ~26 kJ/mol. This result is relatively insensitive to the assumed slope of the low-T portion of the curve; if the steeper slope of Martinez et al.'s prediction (Fig. 6) is used, $\Delta H_{\text{disorder, dolomite}}$ becomes ~23 kJ/mol.

Navrotsky and Capobianco (1987) inferred from their calorimetric study that the enthalpy of disordering is ~14 kJ/mol, and pointed out that because of the quenching problems, this value should be considered as a lower limit. The Landau model of Holland and Powell has $\Delta H_{\text{disorder,dolomite}}$ of ~12 kJ/mol. Subsequently, Navrotsky et al. (1999) derived an enthalpy of complete disordering of 32 ± 5 kJ/mol based on further calorimetric studies. Therefore, the change in slope of this reaction boundary observed in the present study is reasonably consistent with that expected from disordering of the dolomite with increasing temperature. If the low-T (~600 °C) dolomite is truly completely ordered, this study would require the onset of significant disorder to occur only at ~800 °C, higher than predicted by either the Landau model used by Holland and Powell (1998) or the GPA model of Davidson (1994). Alternatively, if the dolomite involved at low T is already partially disordered, the calculated $\Delta H_{\text{disorder, dolomite}}$ would be an underestimate of the actual enthalpy of complete disorder.

Implications for carbonates in the Earth's mantle

The results of this study confirm that the reaction diopside + 2 magnesite = enstatite + dolomite will determine the stable carbonate in lherzolites at temperatures relevant to understanding partial melting in the Earth's mantle, rather than reactions involving magnesite and aragonite (Fig. 8). Aragonite plus magnesite will only be stable at relatively low temperatures, well below the solidus and most models of the geotherm.

Postscript

It may seem that the study of Martinez et al. (1996) was singled out and criticized for the quality of the extrapolation they attempted in their paper. Such was not the intent of this study; it was the intriguing implications of their extrapolation, which was done with the best data then available, that precipitated this study.

Acknowledgements This research was funded by Operating and Research Grants from NSERC. In addition, the multi-anvil laboratory is funded by a MFA grant from NSERC. The author would like to acknowledge with thanks the assistance of D. Caird in both the high-pressure and X-ray laboratories. Official reviews by R. Reeder and P. Ulmer were very helpful and resulted in significant improvements to the manuscript. I acknowledge with thanks discussions with K. Sato in our attempts to reconcile the results of our two studies on this reaction boundary.

References

Bohlen SR (1984) Equilibria for precise pressure calibration and a frictionless furnace assembly for the piston-cylinder apparatus. Neues Jahrb Mineral Monatsh H 9:404–412

Brey G, Brice WR, Ellis DR, Green DH, Harris KL, Ryabchikov ID (1983) Pyroxene–carbonate reactions in the upper mantle. Earth Planet Sci Lett 62:63–74

Buob A, Ulmer P (2000) Stability of dolomite and solid solution between calcium and magnesium carbonates at high pressures and temperatures (Abstr) J Conf Abstr 5:20

Capiobianco C, Burton BP, Davidson PM, Navrotsky A (1987) Structural and calorimetric studies of order-disorder in $CdMg(CO_3)_2$. J Solid State Chem 71:214–223

Chai L, Navrotsky A (1996) Synthesis, characterization, and energetics of solid solution along the dolomite-ankerite join, and implications for the stability of ordered $CaFe(CO_3)_2$. Am Mineral 81:1141–1147

Chatterjee ND, Krüger R, Haller G, Olbricht W (1998) The Bayesian approach to an internally consistent thermodynamic database: theory, database, and generation of phase diagrams. Contrib Mineral Petrol 133:149–168

Dalton JA, Presnall DC (1998) Carbonatitic melts along the solidus of model lherzolite in the system $CaO–MgO–Al_2O_3–SiO_2–CO_2$ from 3–7 GPa. Contrib Mineral Petrol 131:123–135

Davidson PM (1994) Ternary iron, magnesium, calcium carbonates: a thermodynamic model for dolomite as an ordered derivative of calcite-structure solutions. Am Mineral 79:332–339

Domanik KJ, Luth RW (1999) The effect of pressure on thermal gradients in multianvil apparatus. Trans Am Geophys Union 80:S335

Goldsmith JR, Heard HC (1961) Subsolidus phase relations in the system $CaCO_3$–$MgCO_3$. J Geol 69:45–74

Hazen RM, Navrotsky A (1996) Effects of pressure on order-disorder reactions. Am Mineral 81:1021–1035

Holland TJB, Powell R (1990) An internally-consistent thermodynamic dataset with uncertainties and correlations: the system Na_2O–K_2O–CaO–MgO–MnO–FeO–Fe_2O_3–Al_2O_3–SiO_2–TiO_2–C–H_2–O_2. J Metamorph Geol 8:89–124

Holland TJB, Powell R (1998) An internally consistent thermodynamic data set for phases of petrological interest. J Metamorph Geol 16:309–343

Knoche R, Sweeney RJ, Luth RW (1999) Carbonation and decarbonation of eclogites: the role of garnet. Contrib Mineral Petrol 135:332–339

Liu L-G, Lin C-C (1995) High-pressure phase transformations of carbonates in the system CaO–MgO–SiO_2–CO_2. Earth Planet Sci Lett 134:297–305

Luth RW (1993) Diamonds, eclogites, and the oxidation state of the Earth's mantle. Science 261:66–68

Luth RW (1995) Experimental determination of the reaction Dolomite + 2 Coesite = Diopside + 2 CO_2 to 6 GPa. Contrib Mineral Petrol 122:152–158

Martinez I, Zhang J, Reeder RJ (1996) In situ X-ray diffraction of aragonite and dolomite at high pressure and high temperature: evidence for dolomite breakdown to aragonite and magnesite. Am Mineral 81:611–624

McKenzie D, Bickle MJ (1988) The volume and composition of melt generated by extension of the lithosphere. J Petrol 29: 625–679

Navrotsky A, Capobianco C (1987) Enthalpies of formation of dolomite and of magnesian calcites. Am Mineral 72:782–787

Navrotsky A, Dooley D, Reeder R, Brady P (1999) Calorimetric studies of the energetics of order-disorder in the system $Mg_{1-x}Fe_xCa(CO_3)_2$. Am Mineral 84:1622–1626

Putnis A (1992) Introduction to mineral sciences. Cambridge University Press, Cambridge.

Reeder RJ, Nakajima Y (1982) The nature of ordering and ordering defects in dolomite. Phys Chem Mineral 8:29–35

Reeder RJ, Wenk H-R (1983) Structure refinements of some thermally disordered dolomites. Am Mineral 68:769–776

Schultz-Güttler R (1986) The influence of disordered, non-equilibrium dolomites on the Mg-solubility in calcite in the system $CaCO_3$–$MgCO_3$. Contrib Mineral Petrol 93:395–398

Susaki J, Akaogi M, Akimoto S, Shimomura O (1985) Garnet–perovskite transformation in $CaGeO_3$: in-situ X-ray measurements using synchrotron radiation. Geophys Res Lett 12:729–732

Walter MJ, Thibault Y, Wei K, Luth RW (1995) Characterizing experimental pressure and temperature conditions in multianvil apparatus. Can J Phys 73:273–286

Yagi T, Akimoto S (1976) Direct determination of coesite–stishovite transition by in-situ X-ray measurements. Tectonophysics 35:259–270

Zhang J, Martinez I, Guyot F, Gillet P, Saxena SK (1997) X-ray diffraction study of magnesite at high pressure and high temperature. Phys Chem Mineral 24:122–130